

Regulation of Neurofilament Axonal Transport by Phosphorylation in Optic Axons In Situ

Cheolwha Jung and Thomas B. Shea*

*Center for Cellular Neurobiology and Neurodegeneration Research,
Department of Biological Sciences, University of Massachusetts-Lowell*

Axonal transport of neurofilament (NFs) is considered to be regulated by phosphorylation. While existing evidence for this hypothesis is compelling, supportive studies have been largely restricted to correlative evidence and/or experimental systems involving mutants. We tested this hypothesis in retinal ganglion cells of normal mice in situ by comparing subunit transport with regional phosphorylation state coupled with inhibition of phosphatases. NF subunits were radiolabeled by intravitreal injection of ^{35}S -methionine. NF axonal transport was monitored by following the location of the peak of radiolabeled subunits immunoprecipitated from 9×1.1 mm segments of optic axons. An abrupt decline transport rate was observed between days 1 and 6, which corresponded to translocation of the peak of radiolabeled subunits from axonal segment 2 into segment 3. Notably, this is far downstream from the only caliber increase of optic axons at 150μ from the retina. Immunoblot analysis demonstrated a unique threefold increase between segments 2 and 3 in levels of a “late-appearing” C-terminal NF-H phospho-epitope (RT97). Intravitreal injection of the phosphatase inhibitor okadaic acid increased RT97 immunoreactivity within retinas and proximal axons, and markedly decreased NF transport rate out of retinas and proximal axons. These findings provide in situ experimental evidence for regulation of NF transport by site-specific phosphorylation. *Cell Motil. Cytoskeleton* 42:230–240, 1999. © 1999 Wiley-Liss, Inc.

Key words: neurofilaments; axonal transport; phosphorylation; phosphatases; cytoskeleton; axon

INTRODUCTION

Neurofilaments (NFs) are among the most highly phosphorylated proteins within axons. Distinct kinases phosphorylate the N-terminal and C-terminal portions of NFs [Julien and Mushynski, 1983; Pant et al., 1979; Runge et al., 1981; Schekert and Lasek, 1982; Sihag and Nixon, 1989, 1990, 1991] and, in doing so, are thought to modulate aspects of NF assembly and interaction with other cytoskeletal proteins. Like all constituents of the axonal cytoskeleton, NFs are synthesized exclusively within the neuronal perikaryon and are subsequently delivered to the axon by a process referred to as axonal transport [Okabe and Hirokawa, 1992; Nixon, 1993]. The mode of NF axonal transport has not been determined, but, like other aspects of NF behavior, is thought to be regulated by phosphorylation [Lewis and Nixon, 1988;

deWaegh et al., 1992; Komiya et al., 1986; Nixon et al., 1994].

Interpretation of the nature of NF axonal transport during the later periods of their residence within axons remains controversial [Glass and Griffin, 1994; Lasek et al., 1992; Nixon and Logvinenko, 1986]. However, studies thus far commonly describe an overall slowing of the transport rate of NFs during their continued migration

Contract grant sponsor: National Science Foundation.

*Correspondence to: T.B. Shea, Center for Cellular Neurobiology and Neurodegeneration Research, Department of Biological Sciences, University of Massachusetts-Lowell, One University Avenue, Lowell, MA 01854. E-mail: Thomas_Shea@uml.edu

Received 5 October 1998; accepted 8 December 1998

along the axon [Hoffman et al., 1985; Lasek et al., 1992; Nixon and Logvinenko, 1986; Watson et al., 1989]. In myelinated axons, NFs are a major determinant of axonal caliber [deWaegh et al., 1992; Friede and Samorajski, 1970; Hoffman et al., 1984a,b, 1985; Lasek et al., 1983; Nixon et al., 1992; Shea et al., 1992]. The progressive slowing of NFs during transport has been considered to provide for the developmental increase in axonal caliber [Hoffman et al., 1985; Willard and Simon, 1983].

Compelling evidence has been presented that phosphorylation regulates axonal transport of NFs. However, such evidence unfortunately remains largely correlative [Hoffman et al., 1985; Nixon et al., 1994], and/or has been derived from mutant [deWaegh et al., 1992; Watson et al., 1993; Zhang et al., 1997] and cell culture models [Shea et al., 1992]. It would therefore be of interest to demonstrate, in a normal animal, that *in situ* alterations in NF phosphorylation alter NF axonal transport. Moreover, site-specific NF phosphorylation would also be likely to regulate the association of NFs with their putative transport motor system [e.g., Lasek et al., 1992, 1993; Nixon, 1993, 1998; Baas and Brown, 1997]. We present data, obtained in normal mice, indicating that phosphorylation indeed regulates NF axonal transport. Portions of this study have been presented in abstract form [Jung et al., 1997].

MATERIALS AND METHODS

Injection of Radiolabel and Harvesting of Tissues

Murine retinal ganglion cells were radiolabeled *in situ* by injection of 70 μCi ^{35}S -methionine in a total volume of 0.2 μL via a pulled glass capillary pipette into the vitreous of anesthetized mice as described [Nixon and Logvinenko, 1986; Shea et al., 1997]. In some experiments, 100 μM okadaic acid (OA) was included in the injection buffer. While the final concentration of OA in retinal ganglion cells and their axons is impossible to determine, given an internal volume of 12–15 μL of the eye, and making the generous allowance for only half of this volume to be occupied by the lens, injection of 0.2 μL of a 100 μM solution into the vitreous would result in exposure of retinal ganglion cells to a final concentration of 2.67–3.33 μM OA. The level of OA internalized by retinal ganglion cells may be less. Mice were sacrificed by cervical dislocation at intervals of 6 h to 60 days following injection [Nixon and Logvinenko, 1986; Shea et al., 1997]. Briefly, retinas were dissected away from the rest of the eye and optic axons dissected into 9×1.1 mm segments on a glass slide on dry ice. Retinas and segments from five to 11 mice were pooled and homogenized in 1% Triton X-100 in 50 mM Tris (pH 6.9) containing 2 mM EDTA, 1 mM PMSF and 50 $\mu\text{g}/\text{ml}$ leupeptin at 4°C by 50 strokes in a tight-fitting glass-Teflon homogenizer. In some experiments, 100 μM OA

was included in the harvesting and homogenization buffer. The Triton-insoluble cytoskeleton was sedimented by centrifugation 15,000g for 15 min as described [Chiu and Norton, 1982].

Gel Electrophoresis, Autoradiography and Immunoblot Analyses

NF subunits were immunoprecipitated from cytoskeletons, and, in some experiments, from Triton-soluble fractions first clarified of cytoskeletal residue by high-speed centrifugation (100,00g, 1 hr [Shea et al., 1997], by standard methods using a polyclonal antibody (R39; diluted 1:150) that quantitatively immunoprecipitates all three NF subunits, a cocktail of anti-NF polyclonal antisera (H3, M2, and L3; generated in this laboratory to each NF subunit), followed by protein A-sepharose (Sigma) as described [Shea et al., 1990, 1997]. Immunoprecipitated material was subjected to SDS-gel electrophoresis on linear 7% acrylamide gels. Gels were either Coomassie-stained and dried to generate autoradiographs, or separated proteins were transferred to nitrocellulose. Nitrocellulose replicas were probed as described [Shea et al., 1997] with R39 (diluted 1:1,000), the above cocktail of anti-NF polyclonal antisera, monoclonal antibodies directed against phosphorylated (SMI-31) or non-phosphorylated (SMI-32) NF epitopes (Sternberger Monoclonals, Inc., Jarrettsville, MD), a polyclonal antibody (F34) directed against fodrin [Sihag et al., 1996], or a monoclonal antibody (RT97; diluted 1:100) directed against a developmentally delayed, C-terminal phosphoepitope of NF-H [Anderton et al., 1982]. As in our previous studies, pre-immune sera, commercially obtained non-immune sera, or protein A-Sepharose alone did not precipitate of NF polypeptides, and omission of primary antibodies in immunoblot analysis failed to generate reactive species.

Densitometric Analyses and Calculation of Transport Rates

Autoradiographs and nitrocellulose replicas were digitized via a UMax scanner equipped with a transparency adaptor operated by a Macintosh Power PC. Densitometric analyses of digitized images were carried out via NIH Image software by encircling the entire band with the program's freehand selection tool as described previously [Cressman and Shea, 1995]. Since the NF triplet co-migrated along optic axons, we subsequently present densitometric data only for NF-L for simplicity only [e.g., Lasek et al., 1993]. Densitometric calculations using the NF triplet yielded identical relative distributions (not shown). The transport rate of NF subunits, expressed as mm/day was determined for the "50th percentile" of

TABLE I. Percentage Distribution of Radiolabeled NF-L in Optic Axons

Segment	6 h	12 h	24 h	48 h	72 h	6 days	14 days	28 days	60 days
retina	41%	15%	1%	1%	2%	2%	0%	0%	1%
op1	40%	54%	45%	43%	36%	17%	5%	5%	2%
op2	11%	22%	33%	31%	36%	25%	13%	9%	4%
op3	4%	6%	14%	18%	15%	23%	21%	11%	8%
op4	1%	2%	4%	5%	6%	17%	22%	14%	10%
op5	0%	1%	2%	2%	2%	10%	17%	15%	16%
op6	0%	0%	0%	1%	1%	4%	10%	13%	17%
op7	0%	0%	0%	0%	0%	1%	7%	12%	15%
op8	0%	0%	0%	0%	0%	1%	4%	12%	13%
op9	0%	0%	0%	0%	1%	0%	2%	10%	15%

Values represent densitometric analyses of the percentage of NF-L within each segment, where the total radiolabel associated with NF-L in all segments is defined as 100% for each sampling interval. The 50th percentile, defined as that segment into which $\geq 50\%$ of the total radiolabeled NF-L has entered or traversed (see text), is presented in boldface.

radioactivity essentially as described previously [Hoffman et al., 1983] with some modifications (described in detail in Results). The location of the 50th percentile, herein referred to as the “peak,” at various times following injection of radiolabel was operationally defined as that segment into which $\geq 50\%$ of radiolabeled subunits had entered or traversed (e.g., Table I).

Total mean density (density per total area of immunoreactive band) was calculated for autoradiographs and immunoblots. In some occasions (where indicated), integrated mean density (density per area) is also presented for immunoblots. To facilitate comparison of distribution of radiolabeled subunits at different post-injection intervals, total subunit radiolabeled recovered from the retina and all axonal segments was defined as 100% for each respective time interval. The relative amount of radiolabel in each segment was then expressed as a percentage of the total at that interval. The distribution of fodrin was quantified in an identical manner. For immunoblots, total or integrated density is expressed as the fold increase (mean \pm standard error of the mean) obtained for each axonal segment versus that obtained for the retina (obtained by dividing axonal values by those obtained for retinas). All such comparisons were performed for individual autoradiographs and immunoblots, and resultant respective values were then pooled. All tables and graphs of densitometric analyses represent averages derived from autoradiographs derived from at least two independent experiments, and from nitrocellulose replicas of two to five separate experiments, all of which were generated from pools of five to 11 mice per sample in each experiment. Multiple autoradiographs of differing exposures were generated to insure linearity. Similarly, multiple protein loads, antibody concentrations, and intensity

levels during digitization were utilized in immunoblot analyses to insure linearity.

RESULTS

Axonal transport of radiolabeled NF subunits was monitored from 6 h to 60 days post-injection of ^{35}S -methionine radiolabel by autoradiographic analyses of NF subunits immunoprecipitated with a polyclonal antibody (R39) that immunoprecipitates all three NF subunits regardless of phosphorylation state (Fig. 1; see also Jung et al., 1998; Shea et al., 1997). Consistent with previous studies [e.g., Watson et al., 1989; Nixon and Logvinenko, 1986; Lasek et al., 1992, 1993; Jung et al., 1998], transport of NF subunits into optic axons initiated within hours after injection of radiolabel (Fig. 2), and the profile of radiolabeled subunits broadened during continued transport (Fig. 3).

Analysis of NF Transport Rate Along Optic Axons

We monitored the location of the “50th percentile” of radioactivity essentially as described previously [Hoffman et al., 1983]. The location of the 50th percentile, herein referred to as the “peak,” was operationally defined as that segment which $\geq 50\%$ of radiolabeled subunits had entered or traversed. The peak was recovered within segment 1 by 6 h, segment 2 by 24 h, segment 3 by 6 days, segment 4 by 14 days, segment 5 by 28 days, and segment 6 by 60 days post radiolabeling (Table I).

NF subunit transport was further analyzed by calculating the theoretical “maximum transport rate” for the peak. In these analyses, the peak of radiolabeled subunits is assumed to have traversed most/all of the segment in which it is recovered. We also calculated an “average transport rate,” where the peak is considered to have traversed half of the segment in which it is recovered [e.g., Hoffman et al., 1983]. For calculation of maximum and average transport rates, the distances of 1.1 and 0.55 mm, respectfully, were therefore added to the total distance of the 1.1 mm segments through which the peak had migrated. Inherent in both of these calculations is the reasonable assumption that NF subunits have traveled a finite length within that segment from which the peak is recovered. However, since we were concerned about any potential artifactual enhancement of apparent transport rates, we also derived a “minimal transport rate.” For calculation of this rate, no arbitrary distance was applied for the segment in which the peak was recovered, and the distance traversed was calculated using only those segments which the peak had fully traversed. As expected, minor differences exist among the maximum, average and minimum transport rates based on the use of different migratory distances (Fig. 4). Nevertheless, they all demonstrate a dramatic slowing of NF subunit transport rate during the interval from 6 h to

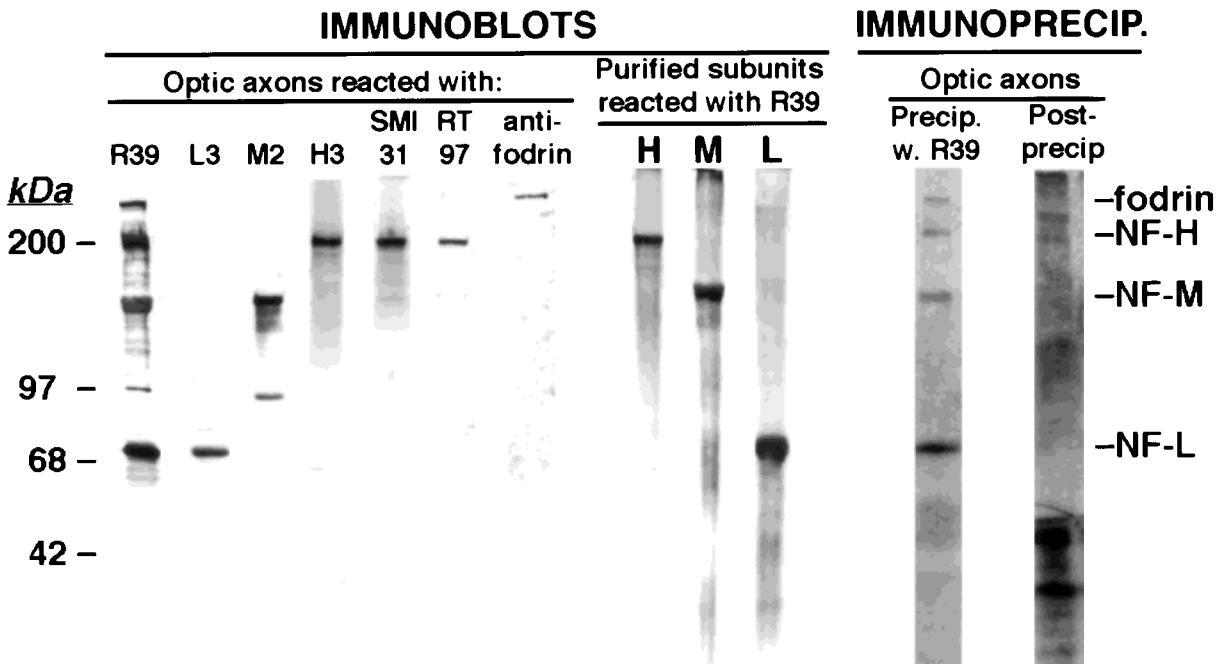


Fig. 1. Characterization of anti-NF polyclonal antibody R39. Panels present nitrocellulose replicas of homogenates of optic axon cytoskeletons and autoradiographs of material immunoprecipitated by R39 from optic axon cytoskeletons 7 days after radiolabeling. As described previously [e.g., Shea et al., 1997], R39 specifically recognizes the NF triplet and fodrin in immunoblot analyses, as demonstrated by comparative probing of nitrocellulose replicas of optic axons with R39,

polyclonal antisera directed against individual NF subunits (H3, M2 and L3), monoclonal antibodies directed against phosphoepitopes of NFs (SMI-31, RT97), and a polyclonal antibody (F34) directed against fodrin, as indicated. Autoradiographs of material immunoprecipitated from radiolabeled cytoskeletons and post-immunoprecipitated material demonstrate that R39 quantitatively immunoprecipitates all three NF subunits and fodrin.

60 days after radiolabel (Fig. 4). In addition to the overall slowing observed along the entire post-injection interval, analyses of subunit transport rate demonstrated a pronounced additional slowing of transport rate between days 3 and 6 after radiolabeling. The peak of radiolabeled subunits entered segment 2 within 24 h and remained there until 3 days after radiolabeling; the peak did not transport into segment 3 until 6 days after labeling (Fig. 4). This regional decrease in subunit transport between days 3 and 6 was further highlighted by calculating transport rates between each segment at all time points after radiolabeling. Subunits underwent an 87% decrease in transport rate between 24 h and 6 days (a total interval of 5 days) following radiolabeling, but only a 37% decrease in transport rate between 6 and 14 days following radiolabeling (an interval of 8 days; Table II). Importantly, while these sequential analyses and comparisons are useful to highlight the differences in regional transport rate, the same conclusion is apparent following visual inspection of autoradiographs themselves (Fig. 2).

An Increase in NF Phosphorylation Is Spatially Associated With the Regionalized Slowing of Transport

The dramatic slowing of NF transport rate observed herein occurred between segments 2 and 3 (Figs. 2, 3;

Table I, II). Since phosphorylation is considered to decrease NF transport rate (above), we examined whether any differences in relative phosphorylation state of NFs could be detected in this region. Densitometric analyses of total NF immunoreactivity in immunoblot analysis using the phospho-independent polyclonal antibody R39 demonstrated an overall proximal-distal increase in total NF immunoreactivity (Fig. 5) as previously described following direct ultrastructural quantitation of NFs [e.g., Nixon and Logvinenko, 1986]. Similar analyses with the relatively restrictive, C-terminal, phospho-dependent monoclonal antibody RT97 also demonstrated an overall proximal-distal increase in NFs phosphorylated at this epitope (Fig. 5). We next compared the integrated immunoreactive densities of R39 and RT97—i.e., intensity per area of the band rather than intensity of total band. Comparison of integrated immunoreactive densities demonstrated two significant regional increases in RT97 immunoreactivity in comparison to that of the retina—one at the initial segment of the axon (which corresponds to the previous demonstration of the onset of NF phosphorylation and the sole increase in axonal caliber; e.g., Nixon et al. [1994]), and the second between segments 2 and 3 (Fig. 5). No further significant increase in RT97 integrated density was observed along the length of the axon (Fig. 5). Increased RT97 immunoreactivity over and

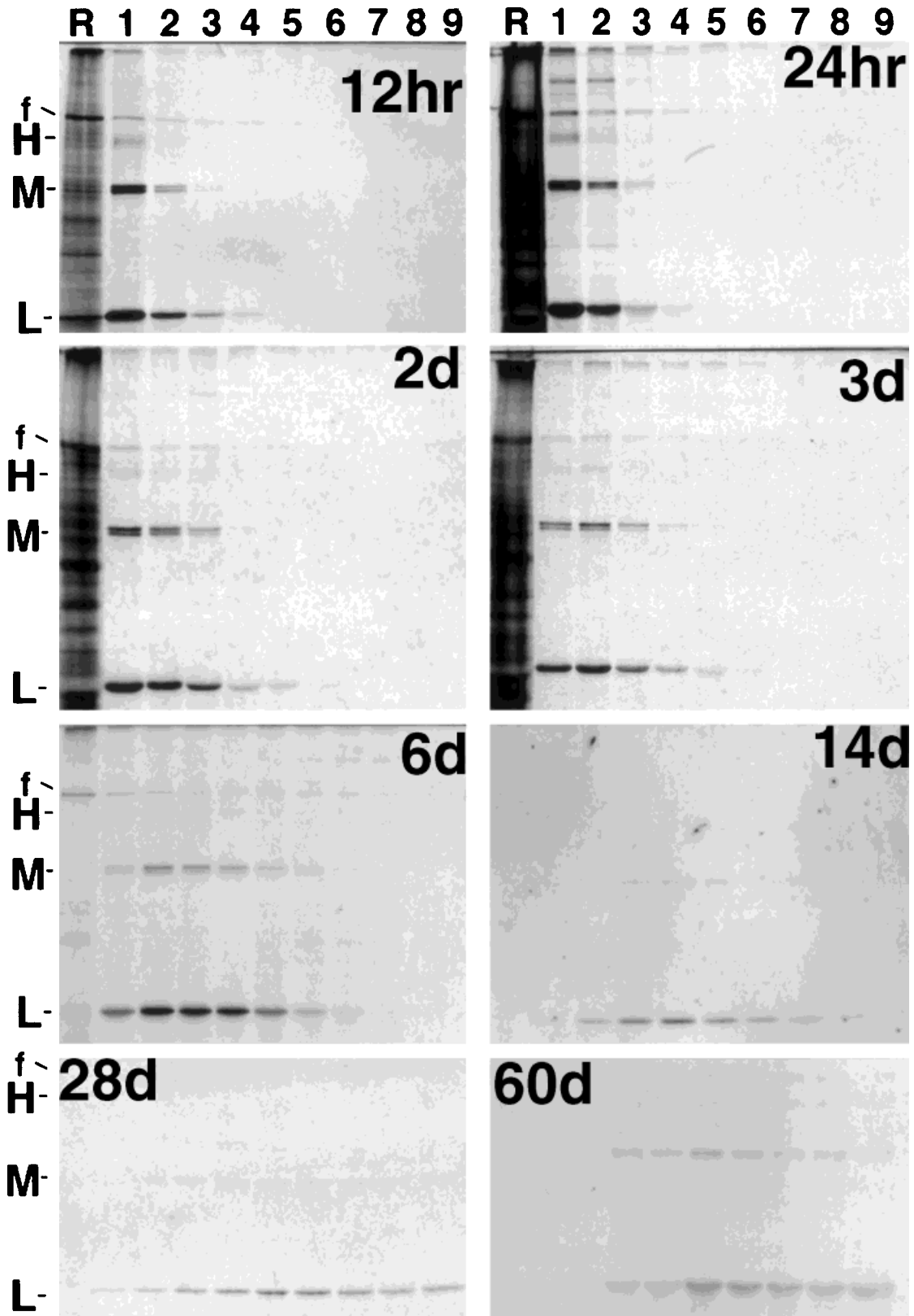


Fig. 2. Autoradiographic analysis of NF axonal transport. Panels present autoradiographs of material immunoprecipitated by R39 from cytoskeletons of retinas (R) and axonal segments (1-9) from 12 h to 60 days post-injection of radiolabel. The migratory positions of 200 kDa

NF-H, 145 kDa NF-M, 70 kDa NF-L and fodrin (f) are indicated. Radiolabeled subunits enter axons within hours after radiolabeling and undergo continued transport along axons.

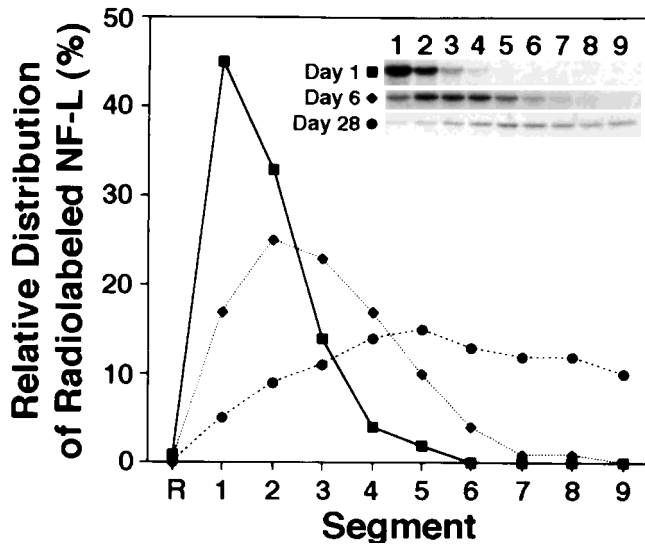


Fig. 3. Distribution of radiolabeled NF subunits. Distribution of radiolabeled NF-L among cytoskeletons from retinas and axonal segments expressed as the percentage of radiolabeled NF-L immunoprecipitated from retinas and each axonal segment, with the total immunoprecipitated NF-L defined as 100% for each time point. As described in previous studies (see text), the peak of transported subunits broadens during continued transport.

above the increase in total 200 kDa immunoreactivity indicates the presence of more of this phospho-epitope per subunit. These analyses indicate that NFs undergo a dramatic increase in site-specific NF-H C-terminal phosphorylation at segment 3. The spatial correlation of this increase in phosphorylation with the observed dramatic slowing of transport rate of radiolabeled NFs leaves open the possibility that NF transport is selectively slowed within this region as a consequence of site-specific phosphorylation.

Inhibition of Phosphatase Activities Increases NF Phosphorylation and Induces Premature Slowing of NF Axonal Transport

We further probed this possibility by *in situ* inhibition of phosphatase activities. This was accomplished by intravitreal injection of OA, previously shown to influence NF phosphorylation in culture [Sacher et al., 1992; Shea et al., 1993]. Immunoblot analyses of retinas and optic axons harvested 7 days after OA injection demonstrated a marked increase in RT97 immunoreactivity within retinas and proximal axonal segments (Fig. 6). This effect resulted from *in situ* inhibition of phosphatase activities rather than artifactual prevention of NF dephosphorylation during isolation, since inclusion of 100 μ M OA in the buffer during harvest of uninjected samples did not increase RT97 immunoreactivity (Fig. 6).

In situ inhibition of phosphatase activities by OA injection also inhibited NF axonal transport (Fig. 7). Prior

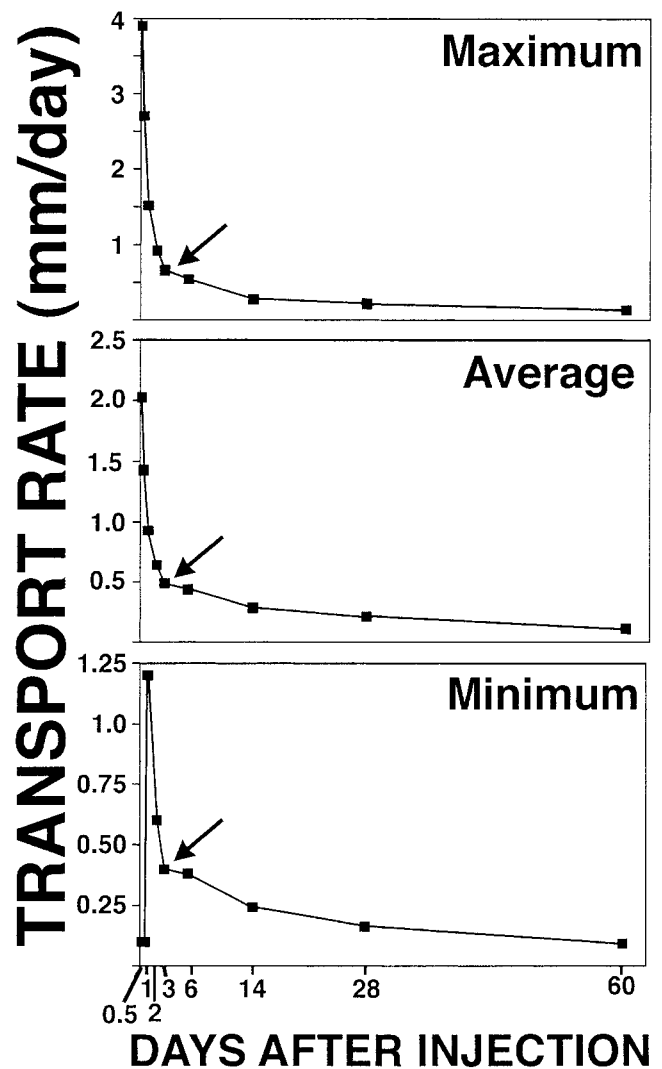


Fig. 4. Regional slowing of the transport rate of NFs in optic axon cytoskeletons. Panels present the maximal, average and minimum transport rate (expressed in mm/day) of the peak (50th percentile) of cytoskeletal radioactive NF-L from 12 h to 60 days calculated as described in Materials and Methods. As described previously (see text), the transport rate of NFs undergo a progressive slowing during continued transport. In addition, a major inflection in the curve of transport rate was noted between days 3 and 6 (arrows), indicating an additional, localized slowing in transport rate.

studies have demonstrated that OA inhibits NF assembly in cultured neurons [Sacher et al., 1992], but does not reduce axonal NFs [Shea et al., 1992]. However, analysis of Triton-soluble fractions confirmed that this was not due to inhibition of NF assembly or incorporation into the cytoskeleton, nor to alterations in steady-state NF levels within cytoskeletons (Fig. 7). Moreover, densitometric analyses revealed that similar levels of radiolabeled NF subunits were present within retinal cytoskeletons (confirming their assembly) in the presence and absence of OA at day 1, yet twice as much radiolabeled NF subunits

TABLE II. Translocation of the Peak of Radiolabeled Subunits From Segment to Segment Along Optic Axons

Interval after injection of radiolabel	Location of peak ^a at start of interval	Location of peak at end of interval	Minimal distance traveled during interval ^b	Transport rate (mm/day) of peak during interval	Percent decline vs. previous ^c interval	Average decline/day ^d during interval
1 day	Retina	segment 2	1.1 mm	1.1	—	—
1–6 days	segment 2	segment 3	1.1 mm	0.22	87%	17%
6–14 days	segment 3	segment 4	1.1 mm	0.14	37%	4.7%
14–28 days	segment 4	segment 5	1.1 mm	0.08	42%	3%
28–60 days	segment 5	segment 6	1.1 mm	0.03	63%	2%

^aDefined as that segment into which $\geq 50\%$ of radiolabeled subunits had entered or traversed (see Table I).

^bIncludes no arbitrary distance for the segment in which the peak was recovered.

^cCalculated by dividing the rate of the current interval by that of the previous interval.

^dCalculated by dividing the decline during each interval by the total days in that interval.

These analyses demonstrate that, while NF subunits undergo a progressive slowing, the most pronounced slowing within axons is observed at the transition between segments 2 and 3.

were retained within OA-treated vs. control retinas at day 6 (indicating impaired translocation out of retinas; Table III). Notably, even if NF assembly and incorporation had been significantly impaired, which they are not, altered distribution of radiolabeled NFs along axons, as seen in Figure 7, would nevertheless indicate that OA impairs axonal transport. Analysis of non-immunoprecipitated homogenates, and of co-precipitated fodrin indicated that this effect was not due to overall inhibition of axonal transport (Fig. 7; Table IV). Premature slowing of NF subunit transport, coupled with increased proximal NF phosphorylation, suggests that a regional increase in phosphorylation is responsible for the dramatic decrease in NF transport rate observed under normal conditions between segments 2 and 3.

DISCUSSION

We have analyzed the early events in axonal transport of radiolabeled NF subunits in murine optic axons *in situ*. Our studies have provided both correlative and experimental evidence that phosphorylation events regulate NF axonal transport. Despite that the majority of NF-H subunits entering optic axons have incorporated sufficient phosphate groups to migrate at 200 kDa on SDS gels, the increase in reactivity with the phospho-dependent antibody RT97 at segment 3 reflects ongoing phosphorylation during axonal transport [see also Komiya et al., 1986; Nixon et al., 1987]. Increased proximal NF phosphorylation at this epitope following intravitreal injection of a phosphatase inhibitor implies that the kinases necessary to mediate this phosphorylation are present and active within retina and proximal regions, but that phosphatase activities normally preclude accumulation of this epitope. This interpretation augments the recent clinical demonstration for increased kinase activity

in the pathogenesis of Amyotrophic lateral sclerosis [Lanius et al., 1995] and the experimental demonstration that kinase activation can induce similar inclusions in cultured motor neurons [Dorodchi and Durham, 1996]. Alternatively, or in addition, the normal relatively fast transport rate of subunits out of the retina and along the proximal 2 axonal segments may preclude significant phosphorylation at the RT97 epitope in these regions. This latter possibility is consistent with previous considerations that the extent of NF-H phosphorylation with perikarya is a function of residence time [Black and Lee, 1988; Koliastos et al., 1989; Shea et al., 1990].

Importantly, the overall behavior of NF subunits in our hands does not differ appreciably from previous reports in murine optic axons. We observed a similar broadening of the peak of radiolabeled subunits during continued transport, and similar overall peak transport rates from 3 to 60 days as reported in previous studies in this system [Lasek et al., 1992; Nixon and Logvinenko, 1986]. These and other [Watson et al., 1989] studies have also noted that subunits underwent initial rapid transport within axons. However, since these previous studies were oriented towards analysis of events occurring during relatively later intervals in subunit transport, early time points were not extensively analyzed. Our comparison of segment-to-segment transport rates during early NF axonal transport, coupled with analysis and manipulation of NF steady-state phosphorylation state within proximal axonal segments, has provided novel insight into the role of phosphorylation in NF axonal transport *in situ*.

The increase in axonal caliber at the lamina cribrosa has been reported to decrease NF axonal transport rate [Griffin et al., 1978, 1983; Hoffman et al., 1985]. However, this increase occurs within the first 150 μ of the axon, and the axonal caliber does not undergo any further increase along the entire axonal length [Nixon and

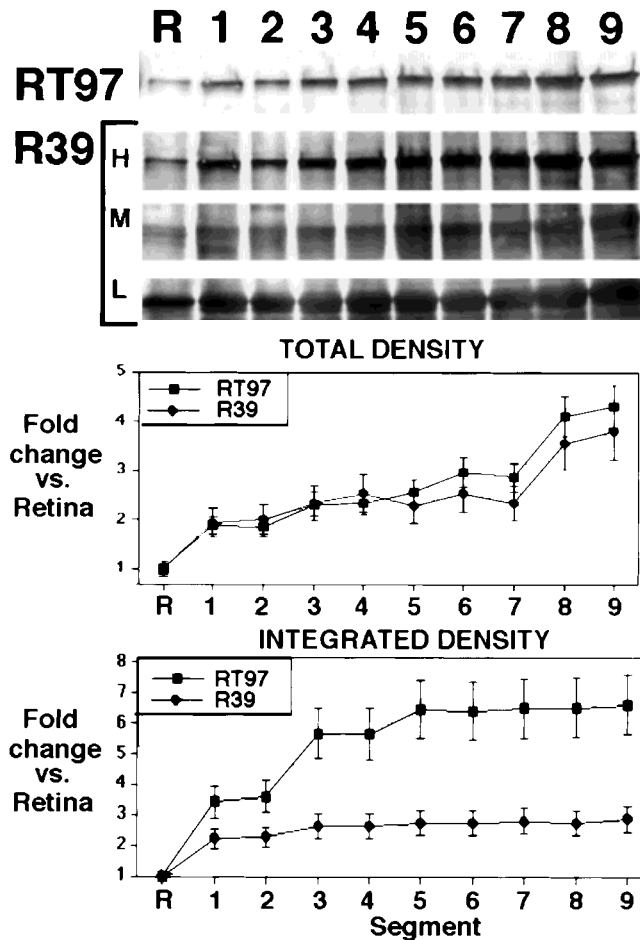


Fig. 5. Regional increase in site-specific NF phosphorylation in proximal optic axons. Panels present nitrocellulose replicas of cytoskeletons from retinas and optic axon segments probed with R39 and RT97 as indicated. The accompanying graphs present the fold increase (calculated for each segment with respect to retinal values) in the total density and integrated density for 200 kDa NF-H for each antibody. Consistent with previous studies (see text), visual inspection and densitometric analyses of replicas reflected a proximal-distal increase in total NF content and an accompanying increase in the RT97 phospho-epitope of NF-H. By contrast, comparison of integrated (mean intensity per area) R39 and RT97 immunoreactive densities demonstrated two significant regional increases in RT97 immunoreactivity—one at the initial segment of the axon in comparison to that of the retina, and the second between segments 2 and 3, with no further significant increase in RT97 phosphorylation along the length of the axon; no such increases were noted for R39. These analyses indicate that NFs undergo a significant increase in site-specific phosphorylation at segment 3 beyond the increase in total NFs.

Logvinenko, 1986; Nixon et al., 1994]. Accordingly, the caliber increase within the initial segment is likely to foster slowing of NF transport rate as subunits initiate axonal transport. However, it is unlikely to be able to contribute to additional downstream changes in NF transport rate between segments 2 and 3 (i.e., over 2 mm downstream of the caliber increase).

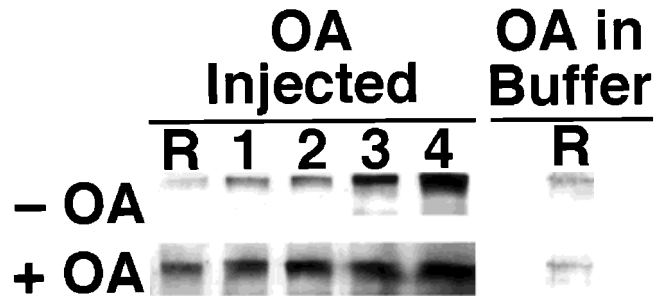


Fig. 6. Inhibition of phosphatase activities increases NF phosphorylation in situ. Panels present nitrocellulose replicas of cytoskeletons of retinas and segments 1–5 of optic axons 6 days following injection of OA or solvent (control). Note that OA markedly increased RT97 immunoreactivity within retinas and segments 1 and 2. Inclusion of 100 μ M OA during homogenization (“OA in buffer”) of uninjected retinas and optic axons did not increase RT97.

NFs undergo axonal transport over a broad range of rates, which has been interpreted to reflect differential association and dissociation of individual NFs with a putative transport motor. That is, the fastest moving NFs would represent those spending relatively more time in association with the motor, while the slowest moving NFs represent those that have dissociated from the motor for relatively longer periods [Lasek et al., 1992, 1993; Nixon, 1993; Baas and Brown, 1997]. The gradual increase in NFs along optic axons ([Nixon and Logvinenko, 1986; Nixon et al., 1992] and shown herein immunologically) could be accomplished by gradual dissociation of NFs from this transport system. Differential association of subunits with a transport motor, and the inverse correlation of this association with extensive C-terminal NF-H phosphorylation, provides a mechanism for the persistence of a portion of radiolabeled subunits along the axon substantially after the majority of subunits have exited the axon [Lasek et al., 1992, 1993; Nixon and Logvinenko, 1986]. Our observation that hypophosphorylated subunits underwent transport at more rapid rates, and were not affected by *in situ* phosphatase inhibition to the same degree as were extensively phosphorylated subunits, suggests that multiple phosphorylation events are required to dissociate NFs from the transport mechanism. This conclusion is supported by the more rapid axonal transport of less phosphorylated variants along optic axons observed herein and in a previous study [Lewis and Nixon, 1988]. In addition, while increased NF phosphorylation in some studies decreased slow axonal transport [Lewis and Nixon, 1988; Griffin and Watson, 1988], NF phosphorylation instead increased transport in studies in the Trembler mutant mouse [deWaegh et al., 1992]. These divergent results prompted the suggestion that the relationship between NF phosphorylation and axonal transport is likely to be complex; some phosphorylation event(s) may

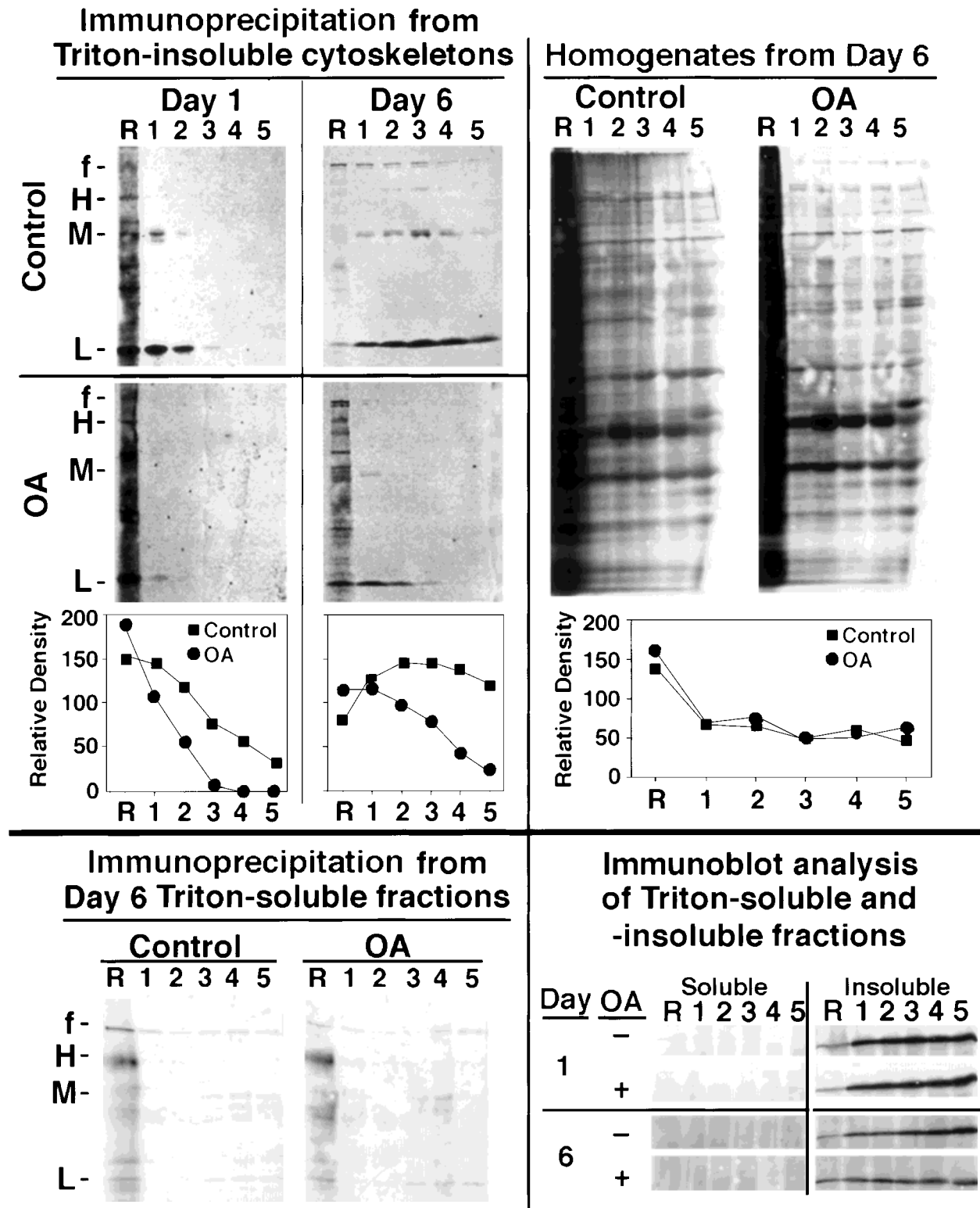


Fig. 7. Phosphatase inhibition slows axonal transport of NFs in optic axons. Panels present autoradiographs of immunoprecipitates from Triton-insoluble cytoskeletons, Triton-soluble fractions, and non-precipitated homogenates from retinas (R) and the first five segments of optic axons 1 and 6 days after intravitreal injection of 100 μ M OA or solvent (control) along with radiolabel. Accompanying graphs present densitometric analyses of the distribution of NF-L in immunoprecipitates from cytoskeletons or of slices of the total lanes of homogenates. Note that OA delayed NF transport, but did not exert a similar effect on the total profile of radiolabeled proteins in optic axons. Note that OA did not induce accumulation of either newly synthesized subunits or

total subunits within Triton-soluble fractions, indicating that the inhibition of NF transport in the presence of OA is not artifactually derived from inhibition of NF assembly; this is further supported by the observation of similar levels of radiolabeled NF subunits within retinal cytoskeletons, which by definition confirms that they have undergone assembly and incorporation into Triton-insoluble structures. The relatively large amount of 200 kDa NF-H that remains within Triton-soluble retinal fractions as immunoprecipitated by R39 has been described previously [Shea et al., 1997]; note that similar levels of this isoform are present within both OA-treated and untreated retinas.

TABLE III. Okadaic Acid Does Not Substantially Inhibit Incorporation of NF Subunits Into Retinal Cytoskeletons, but Inhibits Their Subsequent Transport into Axons

	Day 1 after injection		Day 6 after injection	
	Density ^a	Percent change ^b	Density	Percent change
Control	23520	—	5002	—
OA	20910	-12%	9996	99.8%

^aCalculated as (area of NF-L band) × (integrated density) of autoradiographs such as those presented in Figure 7.

^bCalculated as [(density in OA samples)/(density in control samples)] × 100.

TABLE IV. Phosphatase Inhibition Does Not Diminish Axonal Transport of Fodrin

Axonal segment	Relative distribution (%) of radiolabeled fodrin subunits	
	Control (no OA)	100 μM OA
1	19%	21%
2	20%	20%
3	19%	17%
4	21%	21%
5	21%	21%

Axonal transport of fodrin was analyzed in untreated and 6-day OA-treated mice by immunoprecipitation from axonal cytoskeleton segments 1–5 with R39 (which precipitates fodrin along with NF subunits; e.g., Figure 1). Densitometric analyses of fodrin was carried out identically as described for NFs (see legend for Figure 7). Note that the transport rate of fodrin is not affected by OA. In addition to the demonstration (Fig. 7) that overall axonal transport of radiolabeled proteins in total homogenates is not affected by OA, these data indicate that not all cytoskeletal protein transport is affected by OA.

foster association between NFs, while other event(s) may regulate the coupling of NFs with their putative transport motor [deWaegh et al., 1992; for review, see Pant and Veeranna, 1995]. Our findings are fully consistent with this interpretation. Moreover, our data do not exclude that possibility that regionalized phosphorylation of one or more intermediate “carrier” proteins is responsible for dissociating NFs from the transport complex and therefore decreasing NF transport. We stress, in this regard, that RT97 immunoreactivity only provides an index of increased C-terminal NF-H phosphorylation and conformational alteration of aspects of the C-terminal region of NF-H [for review, see Nixon, 1993, and refs. therein]. It cannot be extrapolated that phosphorylation at the epitope that confers RT97 immunoreactivity represents the same phosphorylation event responsible for dissociating NFs from the putative transport system. In this regard, however, one phosphatase targeted by OA is PP2a, the phosphatase responsible for dephosphorylating C-terminal NF-H regions phosphorylated by the neurofilament

kinase cdk5 [Pant et al., 1997; Veeranna et al., 1995]. These findings leave open the possibility that cdk5-mediated phosphorylation of NF-H sidearms regulates dissociation of NFs from the transport mechanism.

In the present study, detailed analyses of the early stages of NF axonal transport has provided novel correlative and experimental evidence that phosphorylation regulates NF transport *in situ*. Complete analysis of responsible transport systems, kinases/phosphatases, and further studies of site-specific C-terminal NF phosphorylation will provide further insight into the nature and extent of this regulation.

ACKNOWLEDGMENTS

We are grateful to Drs. Scott Brady, Garth Hall and Itzhak Fischer for helpful suggestions and discussions.

REFERENCES

- Anderton BH, Breinburg D, Downes MJ, Green PJ, Tomlinson BE, Ulrich J, Wood JN, Kahn J. 1982. Monoclonal antibodies show that neurofibrillary tangles and neurofilaments share antigenic determinants. *Nature* 298:84–86.
- Baas PW, Brown A. 1997. Slow axonal transport: the polymer transport model. *Trends Cell Biol* 7:380–384.
- Black MM, Lee VM-Y. 1988. Phosphorylation of neurofilament proteins in intact neurons: demonstration of phosphorylation in cell bodies and axons. *J Neurosci* 8:3296–3305.
- Chiu F-C, Norton WT. 1982. Bulk preparation of CNS cytoskeleton and the separation of individual neurofilament proteins by gel filtration: dye-binding characteristics and amino acid compositions. *J Neurochem* 39:1252–1260.
- Cressman CM, Shea TB. 1995. Hyperphosphorylation of Tau and filopodial retraction following microinjection of protein kinase C catalytic subunits. *J Neurosci Res* 42:648–656.
- deWaegh SM, Lee VM-Y, Brady ST. 1992. Local modulation of neurofilament phosphorylation, axonal caliber, and slow axonal transport by myelinating Schwann cells. *Cell* 68:451–463.
- Dorodchi MM, Durham HD. 1996. Activation of protein kinase C induces neurofilament fragmentation, hyperphosphorylation of perikaryal neurofilaments and proximal dendritic swellings in cultured motor neurons. *J Neuropathol Exp Neurol* 55:246–256.
- Friede RL, Samorajski AJ. 1970. Analysis of the process of sheath expansion in swollen nerve fibers. *Brain Res* 19:165–182.
- Glass JD, Griffin JW. 1994. Retrograde transport of radiolabeled cytoskeletal proteins in transected nerves. *J Neurosci* 14:3915–3921.
- Griffin JW, Watson DF. 1988. Axonal transport in neurological disease. *Ann Neurol* 23:3–13.
- Griffin JW, Hoffman PN, Clark AW, Carroll PT, Price DL. 1978. Slow axonal transport of neurofilament proteins: impairment by b,b'-iminodipropionitrile administration. *Science* 202:633–635.
- Griffin JW, Price DL, Hoffman PN. 1983. Neurotoxic probes of the axonal cytoskeleton. *Trends Neurosci* 6:490–495.
- Hoffman PN, Lasek RJ, Griffin JW, Price DL. 1983. Slowing of the axonal transport of neurofilament protein during development. *J Neurosci* 3:1694–1700.
- Hoffman PN, Griffin JW, Price DL. 1984a. Control of axonal caliber by neurofilament transport. *J Cell Biol* 99:705–714.

- Hoffman PN, Griffin JW, Price DL. 1984b. Neurofilament transport in axonal regeneration: implications for the control of axonal caliber. In: Elam J, Cancalon P, editors. *Advances in neurochemistry, axonal transport in growth and regeneration*. New York: Plenum. p 243–260.
- Hoffman PN, Griffin JW, Gold BG, Price DL. 1985. Slowing of neurofilament transport and the radial growth of developing nerve fibers. *J Neurosci* 5:2920–2929.
- Julien JP, Mushynski WE. 1983. The distribution of phosphorylation sites among identified proteolytic fragments of mammalian neurofilaments. *J Biol Chem* 258:4019–4025.
- Jung C, Yabe JT, Wang F-S, Shea TB. 1998. Neurofilaments undergo translocation into axonal neurites before incorporation into Triton-insoluble structures. *Cell Motil Cytoskeleton* 40:44–58.
- Koliastos VE, Applegate MD, Kitt CA, Walker LC, DeLong MR, Price DL. 1989. Aberrant phosphorylation of neurofilaments accompanies transmitter-related changes in rat septal neurons following transection of the fimbria-fornix. *Brain Res* 482:205–218.
- Komiya Y, Tashiro T, Kuokawa M. 1986. Phosphorylation of neurofilament proteins during their axonal transport. *Biomed Res* 7:345–348.
- Lanius RA, Paddon HB, Mezei M, Wagey R, Krieger C, Pelech SL, Shaw CA. 1995. A role for amplified protein kinase C activity in the pathogenesis of amyotrophic lateral sclerosis. *J Neurochem* 65:927–930.
- Lasek RJ, Oblinger MM, Drake PF. 1983. The molecular biology of neuronal geometry: the expression of neurofilament genes influences axonal diameter. *Cold Spring Harbor Symp Quant Biol* 48:731–744.
- Lasek RJ, Paggi P, Katz MJ. 1992. Slow axonal transport mechanisms move neurofilaments relentlessly in mouse optic axons. *J Cell Biol* 117:607–616.
- Lasek RJ, Paggi P, Katz MJ. 1993. The maximum rate of neurofilament transport in axons: a view of molecular transport mechanisms continuously engaged. *Brain Res* 616:58–64.
- Lewis SE, Nixon RA. 1988. Multiple phosphorylated variants of the high molecular mass subunit of neurofilaments in axons of retinal cell neurons: characterization and evidence for their differential association with stationary and moving neurofilaments. *J Cell Biol* 107:2689–2701.
- Nixon RA. 1993. The regulation of neurofilament protein dynamics by phosphorylation: clues to neurofibrillary pathobiology. *Brain Pathol* 3:29–38.
- Nixon RA. 1998. The slow axonal transport of cytoskeletal proteins. *Curr Opin Cell Biol* 10:87–92.
- Nixon RA, Logvinenko KB. 1986. Multiple fates of newly synthesized neurofilament proteins: evidence for a stationary neurofilament network distributed non-uniformly along axons of retinal ganglion cell neurons. *J Cell Biol* 102:647–659.
- Nixon RA, Lewis SE, Marotta CA. 1987. Post-translational modification of neurofilament proteins by phosphate during axoplasmic transport in retinal ganglion cell neurons. *J Neurosci* 7:1145–1158.
- Nixon RA, Logvinenko KB, Sihag RK. 1992. Various cytoskeletal proteins participate with neurofilaments in forming a stationary network in axons. *Mol Biol Cell (Suppl)* 3:173 (abstr).
- Nixon RA, Lewis SE, Mercken M, Sihag RK. 1994. ³²P-orthophosphate and ³⁵S-methionine label separate pools of neurofilaments with markedly different axonal transport kinetics in mouse retinal ganglion cells in vivo. *Neurochem Res* 19:1445–1453.
- Okabe S, Hirokawa N. 1992. Dynamics of neuronal intermediate filaments. *Mol Biol Cell* 3:355 (abstr).
- Pant HC, Veeranna. 1995. Neurofilament phosphorylation. *Biochem Cell Biol* 73:575–592.
- Pant HC, Yoshioka T, Tasaki I. 1979. Divalent cation dependent phosphorylation of proteins in squid giant axon. *Brain Res* 162:303–313.
- Pant AC, Veeranna, Pant HC, Amin N. 1997. Phosphorylation of human high molecular weight neurofilament protein (hNF-H) by neuronal cyclin-dependent kinase 5 (cdk5). *Brain Res* 765:259–266.
- Runge MS, El-Maghrabi MR, Claus TH, Pilkis SJ, Williams RC. 1981. A MAP-2 stimulated protein kinase activity associated with neurofilaments. *Biochemistry* 20:175–180.
- Sacher MG, Athlan ES, Mushynski WE. 1992. Okadaic acid induces the rapid and reversible disruption of the neurofilament network in rat dorsal root ganglion neurons. *Biochem Biophys Res Commun* 186:524–530.
- Schekert G, Lasek RJ. 1982. Neurofilament protein phosphorylation. *J Biol Chem* 257:4788–4795.
- Shea TB, Sihag RK, Nixon RA. 1990. Dynamics of phosphorylation and assembly of the high molecular weight neurofilament protein subunit in NB2a/d1 neuroblastoma. *J Neurochem* 55:1784–1792.
- Shea TB, Paskevich PA, Beermann ML. 1992. The protein phosphatase inhibitor okadaic acid increases axonal neurofilaments and neurite caliber, and decreases axonal microtubules in NB2a/d1 cells. *J Neurosci Res* 35:507–521.
- Shea TB, Dahl D, Nixon RA, Fischer I. 1997. Triton-soluble phospho-variants of the heavy neurofilament subunit in developing and mature mouse central nervous system. *J Neurosci Res* 48:515–523.
- Sihag RK, Nixon RA. 1989. In vivo phosphorylation of distinct domains of the 70-kilodalton neurofilament subunit involves different protein kinases. *J Biol Chem* 264:457–464.
- Sihag RK, Nixon RA. 1990. Phosphorylation of the amino-terminal head domain of the middle molecular mass 145 kDa subunit of neurofilaments: evidence for regulation by second messenger-dependent protein kinases. *J Biol Chem* 265:4166–4171.
- Sihag RK, Nixon RA. 1991. Identification of Ser-55 as a major protein kinase A phosphorylation site on the 70-kDa subunit of neurofilaments: Early turnover during axonal transport. *J Biol Chem* 266:18861–18867.
- Sihag RK, Shea TB, Wang F-S. 1996. Spectrin-actin interaction is required for neurite extension in NB2a/d1 neuroblastoma cells. *J Neurosci Res* 44:430–437.
- Veeranna, Shetty KT, Link WT, Jaffe H, Wang J, Pant HC. 1995. Neurofilament cyclin-dependent kinase-5 phosphorylation sites in neurofilament protein (NF-H) are dephosphorylated by protein phosphatase 2A. *J Neurochem* 64:2681–2690.
- Watson DF, Griffin JW, Fittro KP, Hoffman PN. 1989. Phosphorylation-dependent immunoreactivity of neurofilaments increases during axonal maturation and b,b'-iminodipropionitrile intoxication. *J Neurochem* 53:1818–1829.
- Watson DF, Glass JD, Griffin JW. 1993. Redistribution of cytoskeletal proteins in mammalian axons disconnected from their cell bodies. *J Neurosci* 13:4354–4360.
- Willard M, Simon C. 1983. Modulations of neurofilament axonal transport during the development of rabbit retinal ganglion cells. *Cell* 35:551–559.
- Zhang B, Tu P, Abtahian F, Trojanowski JQ, Lee VM-Y. 1997. Neurofilaments and orthograde transport are reduced in ventral root axons of transgenic mice that express human SOD1 with a G93A mutation. *J Cell Biol* 139:1307–1315.